MicroRNA-139-5p improves sepsis-induced lung injury by targeting Rho-kinase1

XINMIN ZHAO[1,2], MENGMENG WANG[3], ZHAORUI SUN[3], SUYUAN ZHUANG[1], WEI ZHANG[3], ZHIZHOU YANG[1,3], XIAOQIN HAN[3] and SHINAN NIE[1,3]

[1]Department of Emergency Medicine, Jinling Hospital, The First School of Clinical Medicine, Southern Medical University, Nanjing, Jiangsu 210002; [2]Department of Anesthesiology, Yancheng Maternity and Child Health Hospital, Yancheng, Jiangsu 224002, [3]Department of Emergency Medicine, Jinling Hospital, Medical School of Nanjing University, Nanjing, Jiangsu 210002, P.R. China

Received November 5, 2020; Accepted March 24, 2021

DOI: 10.3892/etm.2021.10493

Abstract. Sepsis-induced acute lung injury (ALI) is an inflammatory process that involves inflammatory cytokine production and cell apoptosis. In the present study, the regulatory role of microRNA (miR)-139-5p in sepsis-induced ALI was investigated using a murine model of cecal ligation puncture (CLP) and an *in vitro* model using lipopolysaccharide (LPS)-induced normal human bronchial epithelial cells (NHBEs). Sepsis-induced pathological changes in the lungs of ALI mice were detected using hematoxylin and eosin staining. Lung water content was determined, and the expression of proinflammatory cytokines in the bronchoalveolar lavage fluid and serum of sepsis-induced ALI mice were quantified using ELISA. The levels of oxidative stress in lung tissues were determined using commercial kits. The degree of apoptosis was determined using a TUNEL assay. The expression levels of miR-139-5p and Rho-kinase 1 (ROCK1) were determined using reverse transcription-quantitative PCR and western blot analyses. A dual-luciferase reporter assay was used to confirm the direct targeting of ROCK1 by miR-139-5p. NHBEs were co-transfected with vectors expressing ROCK1 (or empty vector) and miR-139-5p mimics or control mimics prior to LPS treatment. The transcriptional activity of caspase-3, the ratio of apoptotic cells, the expression levels of mucin 5AC, mucin 1, TNF-α, IL-1β, IL-6, NLR family pyrin domain containing 3, apoptosis-associated speck-like protein containing a CARD and caspase-1 were evaluated. Compared with the normal group, mice that underwent CLP exhibited abnormal lung morphology, enhanced production of TNF-α, IL-1β and IL-6, increased reactive oxygen species (ROS), malondialdehyde and lactate dehydrogenase levels, an increased proportion of apoptotic cells and increased ROCK1 expression. Superoxide dismutase, glutathione peroxidase and miR-139-5p levels were decreased following CLP. In the NHBEs, stimulation with LPS caused a marked increase in inflammatory cytokine levels and apoptosis compared with the untreated cells. Overexpression of miR-139-5p attenuated cell apoptosis and inflammation. Overexpression of ROCK1 in NHBEs restored the ROS levels and proinflammatory cytokine production inhibited by miR-139-5p. In conclusion, miR-139-5p alleviated sepsis-induced ALI via suppression of its downstream target, ROCK1, suggesting that miR-139-5p may hold promise in the treatment of sepsis-induced ALI.

Correspondence to: Dr Shinan Nie, Department of Emergency Medicine, Jinling Hospital, Medical School of Nanjing University, 305 Zhongshan East Road, Nanjing, Jiangsu 210002, P.R. China
E-mail: shn_nie@sina.com

Key words: sepsis, acute lung injury, microRNA, Rho-kinase 1, inflammation, apoptosis

Introduction

Sepsis is a complicated disorder that develops as a result of dysregulated host response to infection, may manifest as acute organ dysfunction, and it is associated with a high mortality rate (1). Sepsis is a life-threatening syndrome with a global mortality rate of ~25% (2). Sepsis impairs the function of numerous vital organs, including the brain, kidneys and heart (3-7). Amongst the various sepsis-induced complications, which may result in multiple organ failure, acute lung injury (ALI) is the most likely to occur during the early phase of sepsis, due to the purulent inflammatory involvement of the lungs (8).

Sepsis-induced ALI is characterized by an aggressive inflammatory process that generates inflammatory cytokines and chemokines. The oxidative stress in sepsis-induced ALI is hypothesized to be initiated by the activation of products from lung macrophages and infiltrating neutrophils, and these products rapidly diffuse to the lung epithelial and endothelial cells (9). Redox stress induces production of redox-sensitive transcription factors (such as NF-κB and activator protein-1), leading to increased secretion of proinflammatory cytokines and chemokines, further exacerbating inflammation and oxidative stress (10). Dysregulated lung cell apoptosis is another pathophysiological mechanism implicated in ALI (11). However, there are currently no suitable medications recommended as standard treatment for ALI.

According to a recent genome-wide expression analysis, ~80% of genetic elements are reported to be abnormally expressed in patients with sepsis, with non-coding RNAs, including microRNAs (miRNAs/miRs), long non-coding RNAs (lncRNAs) and circular RNAs, serving as key regulators of the pathogenesis of sepsis (12). miRNAs are ~19-22 nucleotides in length and participate in a wide range of physiological processes by regulating the expression of target genes, and novel therapies that focus on miRNA interventions have been attracting increasing attention (13-15).

miR-139-5p is a critical modulator of the progression of several illnesses, including sepsis. Overexpression of miR-139-5p reduces the levels of IL-1β, IL-6 and TNF-α by inhibiting the activity of NF-κB (16). miR-139-5p has been shown to inhibit the expression of transformation-dependent proteins, thereby regulating hypoxia/ischemia-induced neuronal apoptosis in neonatal rats (17). Additionally, miR-139-5p has also been found to inhibit cell viability and metastasis and induce apoptosis in non-small cell lung cancer (18).

It was previously demonstrated that Rho-kinase 1 (ROCK1) plays a key role in sepsis-induced lung injury, and that the mechanism may involve oxidative and/or nitrosative stress-mediated caspase cleavage, resulting in apoptosis (19). By searching the miRDB database (mirdb.org), ROCK1 was predicted to be a target gene of miR-139-5p. However, the precise effect and regulatory mechanism of miR-139-5p in ALI have yet to be fully elucidated.

In the present study, the regulatory role and potential molecular mechanism of action of miR-139-5p in sepsis-induced ALI were examined using a cecal ligation and puncture (CLP) mouse model, as well as normal human bronchial epithelial cells (NHBEs). The extent of lung tissue damage, apoptosis and expression of inflammatory cytokines were investigated. The results may highlight potential novel therapeutic targets and provide a theoretical basis for the treatment of sepsis-induced ALI.

Materials and methods

Mouse model of CLP-induced sepsis. A total of 20 adult male C57BL/6 mice were purchased from Nanjing Biomedical Research Institute of Nanjing University (Nanjing, China) and reared under normal conditions (temperature 23˚C; humidity 50%; 12/12 h light/dark cycle; lights on at 09:00 am) with free access to food and water. All animals were handled in accordance with the guidelines approved by the Experimentation Ethics Review Committee of Nanjing University. Following acclimation for 1 week, the mice were randomly assigned to two groups: Normal and CLP (n=10 per group). A total of 12 mice underwent electrosurgery to establish a mouse model of sepsis-induced ALI (20,21). Briefly, pentobarbital sodium (50 mg/kg) was injected intraperitoneally to anesthetize the mice, which were then fixed in a supine position on the operating table. A 0.4-cm longitudinal midline incision was performed in the abdomen to expose the cecum. After ligating with a 3-0 silk thread 1 cm from the tip, the cecum was punctured once with a 20-gauge needle, 0.5 cm distal to the ligature. After gently compressing the cecum to squeeze out a small amount of feces, the intestine was repositioned in the abdomen and then sutured. The mice were given a subcutaneous injection of saline immediately after surgery. The same procedure was performed for the normal group, omitting the cecal ligation and puncture. After the mice were awakened following CLP surgery, they were given free access to water and observed under normal conditions for 2 days. At the end of that period, the mice were anesthetized by intraperitoneal injection of sodium pentobarbital (50 mg/kg), 0.2-0.3 ml blood was extracted from the eye, placed at room temperature for 2 h, centrifuged at 1,000 x g for 10 min at 4˚C, and the supernatant was separated and stored in a refrigerator at -80˚C. Following blood collection, pentobarbital sodium (100 mg/kg) was injected intraperitoneally to euthanize the mice, the thorax was cut open to expose the trachea and bronchoalveolar lavage fluid (BALF) was collected.

Hematoxylin and eosin (HE) staining. The HE staining procedure was performed as described previously (22). The lung tissues were immersed in 4% paraformaldehyde solution overnight in 4˚C. Subsequently, the lung tissues were embedded in paraffin, and cut into 5-μm thick serial sections. The tissue sections were dehydrated with an ascending ethanol gradient, cleared using xylene and then stained with hematoxylin solution for 6 min at room temperature, followed by soaking in 1% acidic ethanol and washing with distilled water. Next, the sections were stained with eosin solution for 5 min at room temperature. Finally, the sections were dehydrated with a graded series of alcohol solutions and cleared with xylene. Images were captured using a light microscope (magnification, x400; Olympus Corporation).

Analysis of pulmonary edema. Lung tissue was obtained and weighed, dried at 80˚C, and then weighed again after 48 h to calculate the wet-to-dry (W/D) ratio.

ELISA. TNF-α, IL-6 and IL-1β ELISA kits (cat. nos. 130-101-688, 130-094-065, 130-094-053, respectively) were purchased from Miltenyi Biotec, Inc. ELISA was performed in accordance with the manufacturer's protocol, and absorbance was measured at 450 nm.

Lung tissues were homogenized and diluted to 10%, and centrifuged at 3,000 x g for 10 min at 4˚C. The supernatant was collected in preparation for further analysis. The levels of reactive oxygen species (ROS), malondialdehyde (MDA), lactate dehydrogenase (LDH) and glutathione peroxidase (GSH-px) in the serum and BALF, as well as superoxide dismutase (SOD) levels in the serum, were detected according to the protocol of the manufacturer of the ROS kit (Jianglai Biotech, cat. no. JL20383), lipid peroxidation MDA kit (Beyotime Institute of Biotechnology, cat. no. S0131S), LDH cytotoxicity assay kit (Beyotime Institute of Biotechnology, cat. no. C0016), GSH assay kit (Nanjing Jiancheng Bioengineering Institute, cat. no. S0052) and total SOD assay kit with WST-8 (Beyotime Institute of Biotechnology, cat. no. S0101S), respectively.

TUNEL assay. The 5-μm section of lung tissue embedded in paraffin were dewaxed in the oven at 60˚C for 2 h, washed with xylene at room temperature, rehydrated in a descending alcohol series (100, 90, 80 and 75%) and washed three times with PBS at room temperature. A TUNEL kit (Roche Applied

Science) was to detect apoptotic cells according to the manufacturer's protocol. Cell permeability solution was added for 8 min and 500 μl TUNEL reaction mixture was added (50 μl TdT and 450 μl fluorescein-labeled dUTP) at 37˚C for 1 h in the dark box. After DAPI staining (10 μg/ml; at room temperature for 5 min), the sample was mounted under glass coverslip with a mixture of PBS and glycerol (1:2). Using fluorescence microscopy (magnification, x400; Olympus Corporation), five high-power microscope fields were randomly selected from each glass slide to count the number of TUNEL-positive cells.

RNA extraction and reverse transcription-quantitative (RT-q) PCR analysis. Total RNA from mouse lungs was extracted using the RNA Isolation kit (cat. no. 4992456; Tiangen Biotech, Co., Ltd.) according to the manufacturer's protocol and samples were stored at -80˚C until subsequent use. The PrimeScript™ RT reagent kit (cat. no. DRR037A; Takara Bio, Inc.) was used for the RT of RNA into cDNA using the following conditions: 37˚C for 5 min, 42˚C for 60 min and followed by 70˚C for 10 min. qPCR under the conditions of pre-denaturation at 95˚C for 3 min, 40 cycles of denaturation 95˚C for of 15 sec, annealing at 58˚C for 1 min, and extension at 72˚C for 30 sec was performed using SYBR® Premix Ex Taq™ (Takara Bio, Inc. cat. no. DRR041A). The sequences of the PCR primers used were as follows: MiR-139-5p forward, 5'-TCTACAGTGCACGTGTC-3' and reverse, 5'-GAATAC CTCGGACCCTGC-3'; ROCK1 forward, 5'-TGGAAAGAC ATGCTTGCTCAT-3' and reverse, 5'-CGGTTAGAACAA GAGGTAAAT-3'; mucin (MUC)1 forward, 5'-TGCCGC CGAAAGAACTACG-3' and reverse, 5'-TGGGGTACTCGC TCATAGGAT-3'; MUC5AC forward, 5'-TGCGTCCCACGA CATCTG-3' and reverse, 5'-CAGGTGAATGGGCACATG TG-3 and GAPDH forward, 5'-TTCAACGGCACAGTCAAG G-3' and reverse, 5'-CTCAGCACCAGCATCACC-3' and U6 forward, 5'-CTCGCTTCGGCAGCACA-3' and reverse, 5'-AACGCTTCACGAATTTGCGT-3'. U6 was used as an endogenous control for miR-139-5p and GAPDH was used as a control for other genes. Relative gene expression levels were quantified using the $2^{-\Delta\Delta Cq}$ method (23) and normalized to GAPDH.

Western blotting. Total protein was extracted from lung tissues using the RIPA lysis buffer (Beyotime Institute of Biotechnology). The protein concentration was measured with a bicinchoninic acid protein assay kit (Beyotime Institute of Biotechnology) and equal quantities (30 μg) of protein extract were loaded on a 10% SDS gel. Proteins were resolved using SDS-PAGE and transferred to a PVDF membrane. The membranes were first blocked using fat-free milk (5%) in Tris-buffered saline (TBS) for 2 h at room temperature and then incubated overnight at 4˚C with rabbit monoclonal anti-ROCK1 (cat. no. 4035; 1:1,000; Cell Signaling Technology, Inc.), rabbit monoclonal anti-NLR family pyrin domain containing 3 (anti-NLRP3; cat. no. 15101; 1:1,000; Cell Signaling Technology, Inc.), rabbit monoclonal anti-apoptosis-associated speck-like protein containing a CARD (anti-ASC; cat. no. 67824; 1:1,000; Cell Signaling Technology, Inc.), rabbit monoclonal anti-caspase-1 (cat. no. 24232; 1:1,000; Cell Signaling Technology, Inc.), rabbit monoclonal anti-caspase-3 (cat. no. 9662; 1:1,000; Cell Signaling Technology, Inc.) and anti-cleaved caspase-3 (cat. no. 9661; 1:1,000; Cell Signaling Technology, Inc.), rabbit monoclonal anti-Bcl-2 (cat. no. 4223; 1:1,000; Cell Signaling Technology, Inc.), rabbit monoclonal anti-Bax (cat. no. 14796; 1:1,000; Cell Signaling Technology, Inc.) or rabbit polyclonal anti-GAPDH (cat. no. sc-32233; 1:2,000; Santa Cruz Biotechnology, Inc.), and subsequently with horseradish peroxidase-conjugated goat anti-rabbit IgG antibody (cat. no. 98164; 1:2,000; Cell Signaling Technology, Inc.) for 2 h at room temperature. The optical density values of all bands were standardized to the respective GAPDH band and visualized using luminescent reagents (Santa Cruz Biotechnology, Inc.) and analyzed via ImageJ software 1.4 (National Institutes of Health).

Dual-luciferase reporter assay. The ROCK1 3'-untranslated region (3'-UTR) fragment with a putative binding site for miR-139-5p obtained from ensemble database (version 38; https://asia.ensembl.org;) was entered into the Primer3Plus website (https://www.bioinformatics.nl/cgi-bin/primer-3plus/primer3plus.cgi) to acquire the primer sequences, which was cloned into the luciferase gene in a pmirGlo vector (Shanghai GenePharma, Co., Ltd.) by Shanghai GenePharma, Co., Ltd. Mutant (MUT) ROCK1 3'-UTR was used to construct the ROCK1-MUT vector. 293 cells obtained from The Cell Bank of Type Culture Collection of The Chinese Academy of Sciences ($5x10^4$ cells/well) were plated in 12-well plates (Thermo Fisher Scientific, Inc.) with 10% FBS and 1% penicillin/streptomycin in a humidified incubator at 37˚C with 5% CO_2 and co-transfected with miR-139-5p mimics (50 nM, 5'-UCUACAGUGCACGUGUCUCCAGU-3') or negative control (NC) mimics (50 nM, 5'-UUUGUACUACAC AAAAGUACUG-3') and ROCK1-wild type (WT, 100 ng) or ROCK1-MUT (100 ng) when they reached 70-80% confluence. Luciferase activity was assessed using a Dual-Luciferase Reporter assay system (Promega Corporation) 2 days post-transfection and normalized to that of *Renilla* luciferase activity.

Cell culture. NHBE cells were purchased from The Cell Bank of Type Culture Collection of The Chinese Academy of Sciences. NHBE cells were cultured in DMEM (Invitrogen; Thermo Fisher Scientific, Inc.) with 10% FBS and 1% penicillin/streptomycin in a humidified incubator at 37˚C with 5% CO_2. The six cell groups were as follows: i) Control, ii) LPS, iii) LPS plus miR-NC mimics, iv) LPS plus miR-139-5p mimics, v) LPS plus miR-139-5p mimics and empty vector and vi) LPS plus miR-139-5p mimics and overexpression (Ov)-ROCK1. miR-139-5p mimics (5'-UCUACAGUGCAC GUGUCUCCAGU-3'; 50 nM) and control mimics (5'-UUU GUACUACACAAAAGUACUG-3'; 50 nM) were prepared by Shanghai GenePharma Co., Ltd., and transfected into NHBE cells using Lipofectamine® 2000 (Invitrogen; Thermo Fisher Scientific, Inc.). At 24 h post-transfection, cells were treated with 1 mg/ml lipopolysaccharide (LPS; Sigma-Aldrich; Merck KGaA). miR-139-5p, IL-1b, IL-6 and ROCK1 levels were assessed 6 h after LPS treatment. The ROCK1 overexpression plasmid (OV) was established into the pcDNA3.1 vector (Invitrogen; Thermo Fisher Scientific, Inc.), whereas an empty vector served as the Vector. NHBEs were co-transfected with 1 μg Ov-ROCK1 (or Vector) and 50 nM

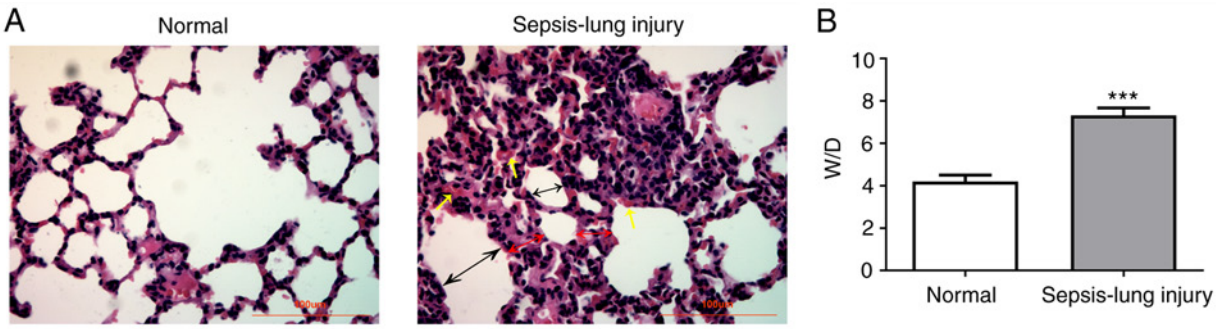

Figure 1. Pathological changes in the lung tissues. (A) Representative histological images of hematoxylin and eosin staining (magnification, x400). Yellow single arrows represent inflammatory cells, black double arrows represent alveolar cavities, and red double arrows represent alveolar septa. Scale bar, 100 μm. (B) W/D weight ratio of the lung in mice 24 h after surgery. Data are presented as the mean ± standard deviation. ***P<0.001 vs. normal group. W/D, wet/dry.

miR-139-5p mimics 24 h prior to treatment with LPS using Lipofectamine® 2000 (Invitrogen; Thermo Fisher Scientific, Inc.). NHBEs co-transfected with empty vector and control mimics were used as the respective controls.

Cell apoptosis assay. Cells were seeded (1x10^6 cells/well) in six-well plates and placed in an incubator for 12 h, followed by another 48 h of incubation after transfection, as described above. Next, cells were digested, washed twice with PBS and incubated in 1X binding buffer (provided in the Annexin V-FITC/PI apoptosis kit; cat. no. C1062M; Beyotime Institute of Biotechnology), adjusting the cell concentration to 1x10^6/ml. Subsequently, 10 μl Annexin V-FITC and 5 μl propidium iodide (PI) were added to the cells (200 μl) and cells were incubated for 15 min at room temperature in the dark. BD FACSCalibur™ flow cytometer (BD Biosciences) was used to quantify stained cells and data were analyzed by FlowJo software (version 7.6.1; FlowJo LLC).

Statistical analysis. All experiments were repeated three times, and the data are presented as the mean ± standard deviation. Comparisons between two groups were performed using a unpaired Student's t-test. Comparisons between multiple groups were performed using one-way ANOVA followed by Tukey's post hoc test. All data were analyzed using GraphPad Prism version 7.0 (GraphPad Software, Inc.). P<0.05 was considered to indicate a statistically significant difference.

Results

Lung histological analysis. To investigate the effects of miR-139-5p in the regulation of sepsis-induced ALI, a mouse model of sepsis was established by CLP surgery. The results of lung tissue histological examination are shown in Fig. 1. No pathological changes were observed in the normal group (Fig. 1A). However, serious injury was present in the sepsis group compared with the normal control group, where the normal alveolar structure of the lung injury group was partially destroyed, inflammatory cells infiltrated, alveolar septum was significantly thickened, alveolar cavity was narrowed, and some alveoli were atrophied. In addition, the sepsis group had a significantly higher W/D ratio compared with the normal group (Fig. 1B). These results indicated that the ALI mouse model was successfully established.

Inflammatory cytokines in the serum and BALF, and oxidative stress. In the normal group, TNF-α, IL-6 and IL-1β were maintained at low levels in the serum and BALF (Fig. 2A and B). However, the expression levels of TNF-α, IL-6 and IL-1β were significantly increased following CLP, suggesting a notable increase in the release of inflammatory factors.

Oxidative stress levels were analyzed by measuring the ROS levels in the lung tissues (Fig. 2C) and measuring SOD, GSH-px, MDA and LDH activity (Fig. 2D). ROS levels were increased in septic mice compared with the normal group. Furthermore, the SOD and GSH-px activities were notably reduced in septic mice compared with the controls. By contrast, MDA and LDH activities were higher in the sepsis group compared with the normal group. These results suggested that the levels of inflammatory factors and oxidative stress in the serum and BALF were upregulated in mice following sepsis-induced lung injury.

Apoptosis and inflammation in lung tissues. Lung tissue sections were stained using TUNEL reagent to examine apoptotic cell death. An increased number of TUNEL-positive (apoptotic) cells were detected in mice with sepsis-induced lung injury compared with the normal group (Fig. 3A). The results suggested that sepsis-induced ALI promoted cell apoptosis.

Expression of miR-139-5p and ROCK1 in lung tissues. Next, the levels of miR-139-5p were analyzed by RT-qPCR, and the results revealed that miR-139-5p levels were decreased in the sepsis-induced lung injury group compared with the normal group (Fig. 3B). ROCK1 expression was detected by RT-qPCR and western blot analyses and was found to be significantly upregulated in the sepsis-induced lung injury group compared with the normal group (Fig. 3C and D).

miR-139-5p targets ROCK1. The predicted binding site between ROCK1 3'-UTR and miR-139-5p is shown in Fig. 4A. WT and MUT luciferase reporter gene plasmids containing the 3'-UTR region of ROCK1 were created and co-transfected with miR-139-5p mimics and mir-NC. Dual-luciferase reporter experiments demonstrated that the luciferase activity of ROCK1-WT was significantly reduced in cells transfected with miR-139-5p compared with the control mock cells. These findings indicated that ROCK1 regulates the expression of its downstream target, miR-139-5p (Fig. 4).

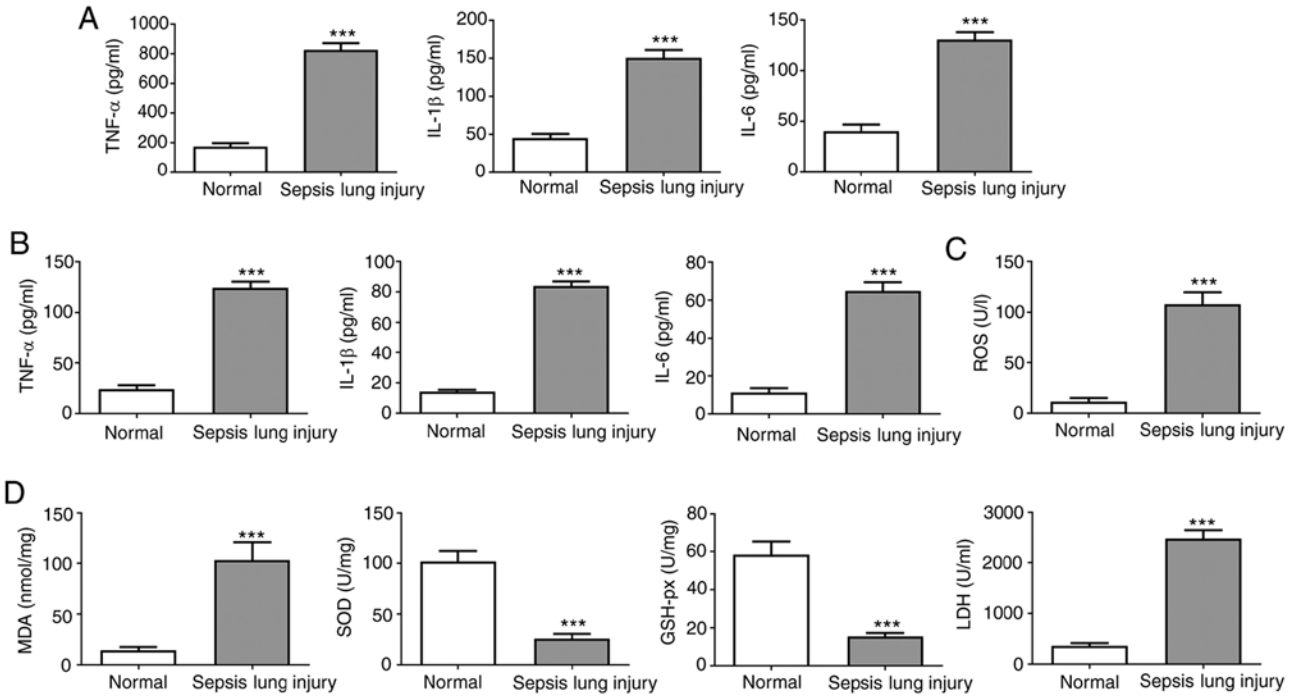

Figure 2. Effect of induction of ALI on the expression of inflammatory factors. (A) IL-1β, TNF-α and IL-6 serum levels were assessed by ELISA. (B) IL-1β, TNF-α and IL-6 BALF levels were evaluated by ELISA. (C) ROS levels in mouse lung tissues were measured using commercial ROS assay kits. (D) MDA, SOD, LDH and GSH-px activity in mouse lung tissues was evaluated using commercial assay kits. Data are presented as the mean ± standard deviation. ***P<0.001 vs. normal group. ALI, acute lung injury; SOD, superoxide dismutase; MDA, malondialdehyde; LDH, lactate dehydrogenase; GSH-px, glutathione peroxidase; BALF, bronchoalveolar lavage fluid; ROS, reactive oxygen species.

miR-139-5p overexpression inhibits LPS-induced inflammation and oxidative stress via targeting ROCK1 in NHBEs. In order to further determine the beneficial effects of miR-139-5p overexpression on sepsis-induced lung injury, an *in vitro* NHBE cell model was developed to mimics *in vivo* sepsis-induced epithelial cell stimulation using LPS. miR-139-5p mimics were transfected into NHBE cells, and RT-qPCR was used to confirm overexpression. Compared with the control group, the expression of miR-139-5p was significantly decreased in the LPS-treated group, whereas transfection of miR-139-5p mimics prior to LPS treatment significantly increased the levels of miR-139-5p in NHBEs (Fig. 5A). Next, ROCK1 overexpression plasmid was transfected in NHBE cells, and overexpression was confirmed using both RT-qPCR and western blotting. Compared with the control group, the expression of ROCK1 was significantly increased in the Ov-ROCK1 group and the Vector group (Fig. 5B and C).

MUC5AC and MUC1 are markers of lung mucosal epithelial cell damage (24). To further explore whether miR-139-5p modulates inflammation and oxidative stress by specifically targeting ROCK1, NHBEs were co-transfected with miR-139-5p mimics and vectors expressing ROCK1 (or empty vector). LPS-treated cells exhibited significantly higher levels of MUC5AC and MUC1 compared with the untreated cells. The NHBEs transfected with control mimics exhibited similar levels of MUC5AC and MUC1, whereas transfection of miR-139-5p mimics significantly decreased the expression of MUC5AC and MUC1. Compared with the miR-139-5p mimics group, there were no differences between miR-139-5p and empty vector co-transfected NHBEs, whereas miR-139-5p and Ov-ROCK1 co-transfected NHBEs exhibited significantly increased expression of MUC5AC and MUC1 (Fig. 6A). The levels of inflammatory factors in the cell supernatants were assessed using ELISA. Compared with the control group, the expression of TNF-α, IL-1β and IL-6 were significantly increased by LPS treatment. Overexpression of miR-139-5p largely suppressed the production of pro-inflammatory cytokines in NHBEs, whereas ROCK1 overexpression resulted in significant upregulation of TNF-α, IL-1β and IL-6 at the protein level (Fig. 6B).

Next, the protein expression levels of NLRP3, ASC and caspase-1 were examined and found to be significantly increased following LPS treatment compared with the control group (P<0.05). miR-139-5p mimics transfection alone or co-transfection with the empty vector control resulted in significant decreases in NLRP3, ASC and caspase-1. However, cells co-transfected with miR-139-5p mimics and Ov-ROCK1 exhibited significant increases in the expression of NLRP3, ASC and caspase-1 (Fig. 6C). These data suggest that miR-139-5p inhibits the expression of inflammatory factors in NHBEs cells by targeting ROCK1.

To determine the effects of miR-139-5p and ROCK1 on oxidative stress, the levels of indicators of ROS were detected. Compared with the control group, LPS treatment significantly increased the levels of ROS; miR-139-5p mimics and miR-139-5p mimics co-transfection with empty vector control resulted in significant decreases in the levels of ROS. However, miR-139-5p mimics co-transfection with Ov-ROCK1 resulted in a significant increase in the levels of ROS (Fig. 6D). Additionally, the levels of SOD, GSH-px, MDA and LDH were determined. The changes in expression of MDA and LDH

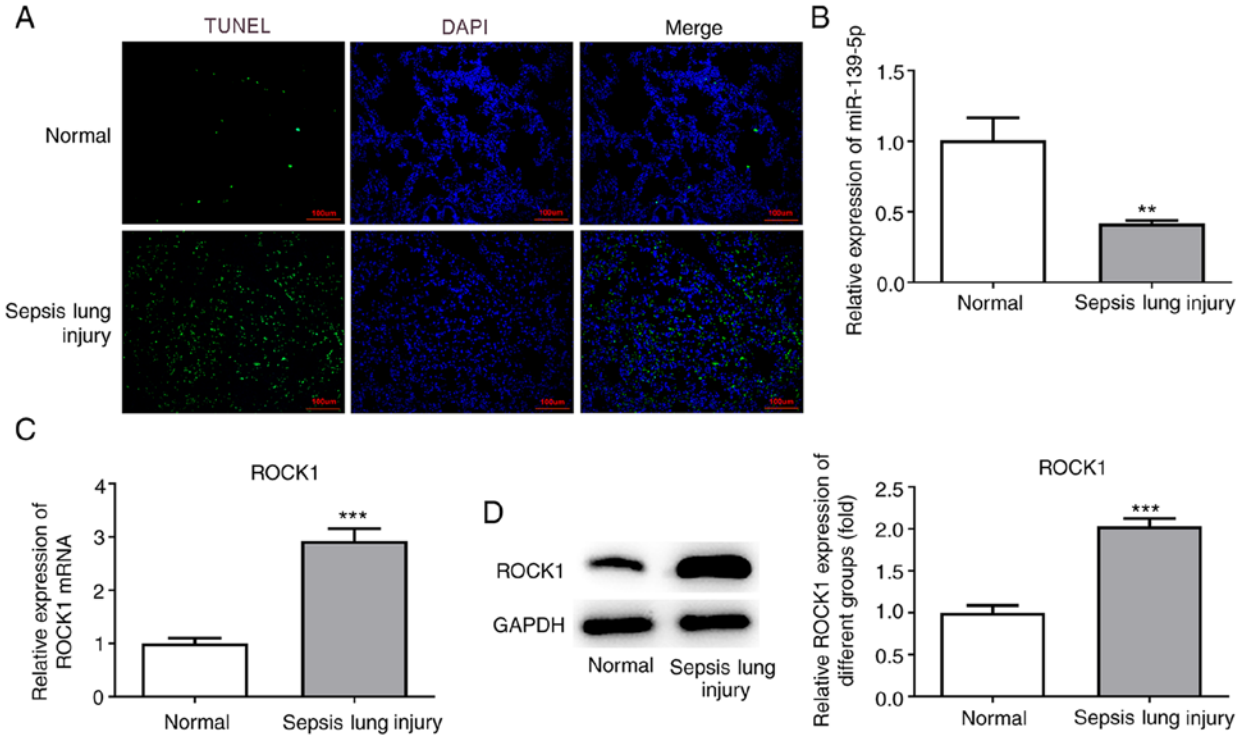

Figure 3. Effects of ALI induction on cell apoptosis, and the expression of miR-139-5p and ROCK1. (A) Histological analysis of mouse lung tissue samples using TUNEL staining. Representative histological images (magnification, x400) and percentage of positively stained cells. Scale bar, 100 μm. (B) miR-139-5p levels in lung tissues were assessed using RT-qPCR analysis. ROCK1 levels in lung tissues were assessed by (C) RT-qPCR and (D) western blotting. Data are presented as the mean ± standard deviation. **P<0.01, ***P<0.001 vs. normal group. RT-qPCR, reverse transcription-quantitative PCR; ALI, acute lung injury; ROCK1, Rho-associated kinase 1; miR, microRNA.

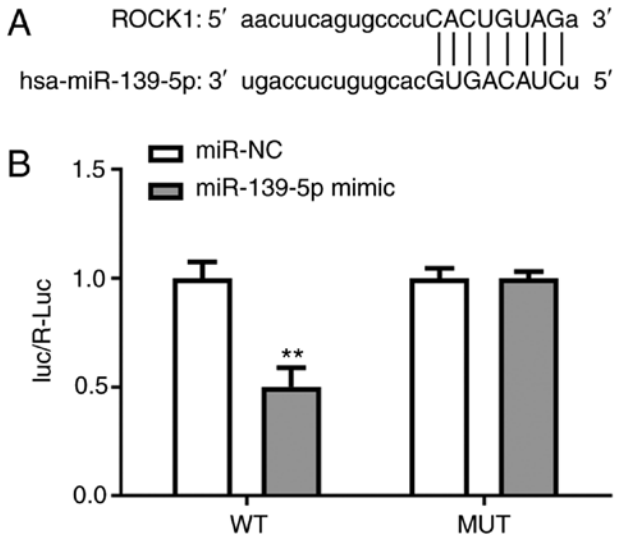

Figure 4. ROCK1 is a direct target of miR-139-5p. TargetScan predicted that ROCK1 was a direct downstream target of miR-139-5p. (A) Putative ROCK1 binding site on miR-139-5p (ROCK1-WT). (B) 293T cells were co-transfected with NC mimics or miR-139-5p mimics with ROCK1-WT or ROCK1-MUT. **P<0.01 vs. miR-NC. ROCK1, Rho-associated kinase 1; miR, microRNA; WT, wild-type; MUT, mutant; NC, negative control.

were the same as those of ROS, whereas SOD and GSH-px levels exhibited the opposite trend. Compared with the control group, LPS treatment significantly decreased the levels of SOD and GSH-px; miR-139-5p mimics and miR-139-5p mimics co-transfected with the empty vector control significantly increased, whereas miR-139-5p mimics co-transfected with Ov-ROCK1 significantly decreased the levels of SOD and GSH-px (Fig. 6E). Taken together, these findings indicated that miR-139-5p overexpression may inhibit LPS-induced inflammation and oxidative stress via targeting ROCK1 in NHBEs.

miR-139-5p reduces apoptosis via suppression of ROCK1 expression in NHBEs. To further examine whether miR-139-5p regulated cell apoptosis by targeting ROCK1, NHBEs were co-transfected with miR-139-5p mimics and vector expressing ROCK1 (or empty vector control). The LPS-treated cells exhibited a markedly higher rate of apoptosis compared with the control cells. The NHBEs transfected with miR-NC exhibited a similar rate of apoptosis as the LPS group, whereas transfection with miR-139-5p mimics significantly decreased the proportion of apoptotic cells. NHBEs transfected with miR-139-5p mimics and empty vector control had a similar proportion of apoptotic cells as that of the miR-139-5p mimics group; however, miR-139-5p mimics and Ov-ROCK1 co-transfection significantly increased the proportion of apoptotic NHBEs (Fig. 7A).

Furthermore, the levels of key proteins associated with the apoptotic pathway were measured. The levels of Bax and cleaved caspase-3 were higher in LPS-treated NHBEs as well as in LPS-treated NHBEs transfected with miR-NC compared with NHBEs with miR-139-5p mimics and empty vector co-transfection. Compared with the miR-139-5p mimics and empty vector co-transfection groups, the expression of Bax and cleaved caspase-3 were increased in the miR-139-5p mimics plus Ov-ROCK1 group. However, the Bcl-2 protein levels in the

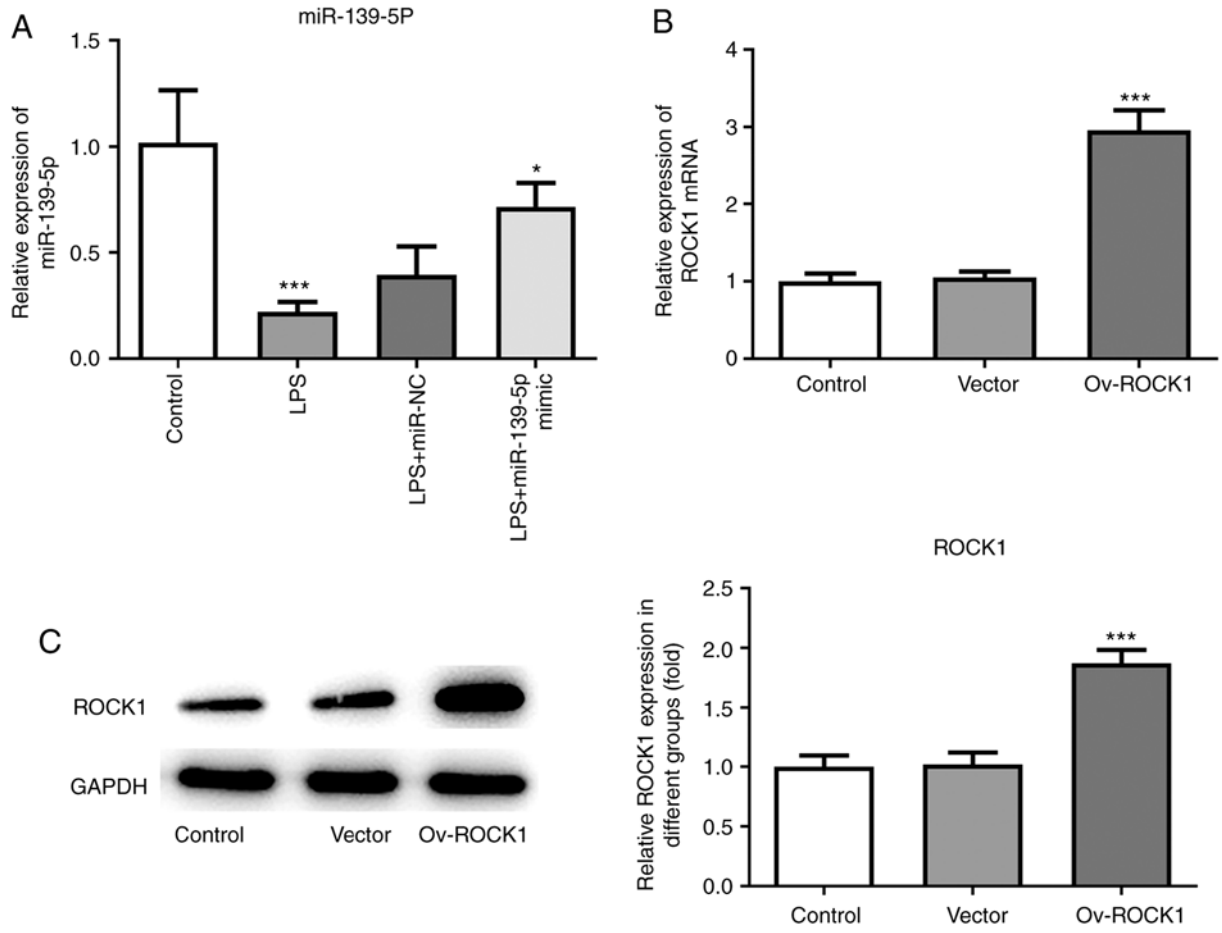

Figure 5. Effects of transfection with miR-139-5p mimics and Ov-ROCK1 on the expression of miR-139-5p and ROCK1 in LPS-stimulated NHBEs. (A) NHBEs were transfected with miR-NC mimics or miR-139-5p mimics and subsequently treated with LPS. The relative expression of miR-139-5p was examined using RT-qPCR. NHBEs were transfected with the empty vector control or Ov-ROCK1 and the expression levels of ROCK1 were analyzed using (B) RT-qPCR and (C) western blotting. Data are presented as the mean ± standard deviation. ***P<0.001 vs. normal (control) group; *P<0.01 vs. LPS + miR-NC. ROCK1, Rho-associated kinase 1; miR, microRNA; RT-qPCR, reverse transcription-quantitative PCR; NHBEs, normal human bronchial epithelial cells; Ov, overexpression; LPS, lipopolysaccharide.

LPS group were significantly decreased compared with those in the control group, and the miR-139-5p mimics and vector co-transfection group exhibited significant decreases in Bcl-2 protein levels compared with the miR-139-5p mimics, as well as the miR-139-5p mimics and empty vector co-transfection group (Fig. 7B). These results suggested that miR-139-5p may inhibit cell apoptosis via suppression of ROCK1 expression in NHBEs.

Discussion

Sepsis-induced ALI is a clinical syndrome characterized by injury of alveolar epithelial and endothelial cells (25). ALI is a condition that develops from excessive inflammation, and involves a variety of potential therapeutic targets and signaling pathways (26). The pathophysiology of human sepsis is similar to that caused by cecal perforation in the mouse CLP model, and it has been widely used to study organ dysfunction caused by sepsis (27). In the present study, a mouse model of sepsis-induced ALI was successfully established, and the mice exhibited alveolar wall thickening and pulmonary edema.

miR-139-5p has been identified as a tumor suppressor, and acts by reducing cell migration, invasion and metastasis in breast, colorectal, prostate and esophageal squamous cell carcinomas (28-31). In addition, miR-139-5p is involved in the regulation of multiple DNA repair and ROS defense pathways, and is a potent regulator of the breast cancer response to radiotherapy (32). Furthermore, deficiency of miR-139-5p was shown to result in the initiation of the MAPK, NF-κB and STAT3 signaling pathways, thereby contributing to the development of intestinal inflammation and colorectal cancer (33). Therefore, in the present study, the effects of miR-139-5p on lung injury, oxidative stress, inflammation and autophagy were assessed, and the molecular mechanisms in a mouse model of CLP-induced ALI were determined. In the *in vivo* model, sepsis-induced ALI resulted in a significant increase in the levels of inflammatory cytokines, oxidative stress and apoptosis compared with the normal mice. Additionally, miR-139-5p levels were decreased in mice with septic lung injury.

ROCK1 has been reported to interact with miRNAs and lncRNAs during cancer pathogenesis to regulate cell migration, invasion and metastasis. For example, miR-202-5p was found to inhibit tumor cell migration and invasion in osteosarcoma, whereas upregulation of ROCK1 abrogated these effects (34). In the present study, ROCK1 was predicted and confirmed to be a direct downstream target of miR-139-5p.

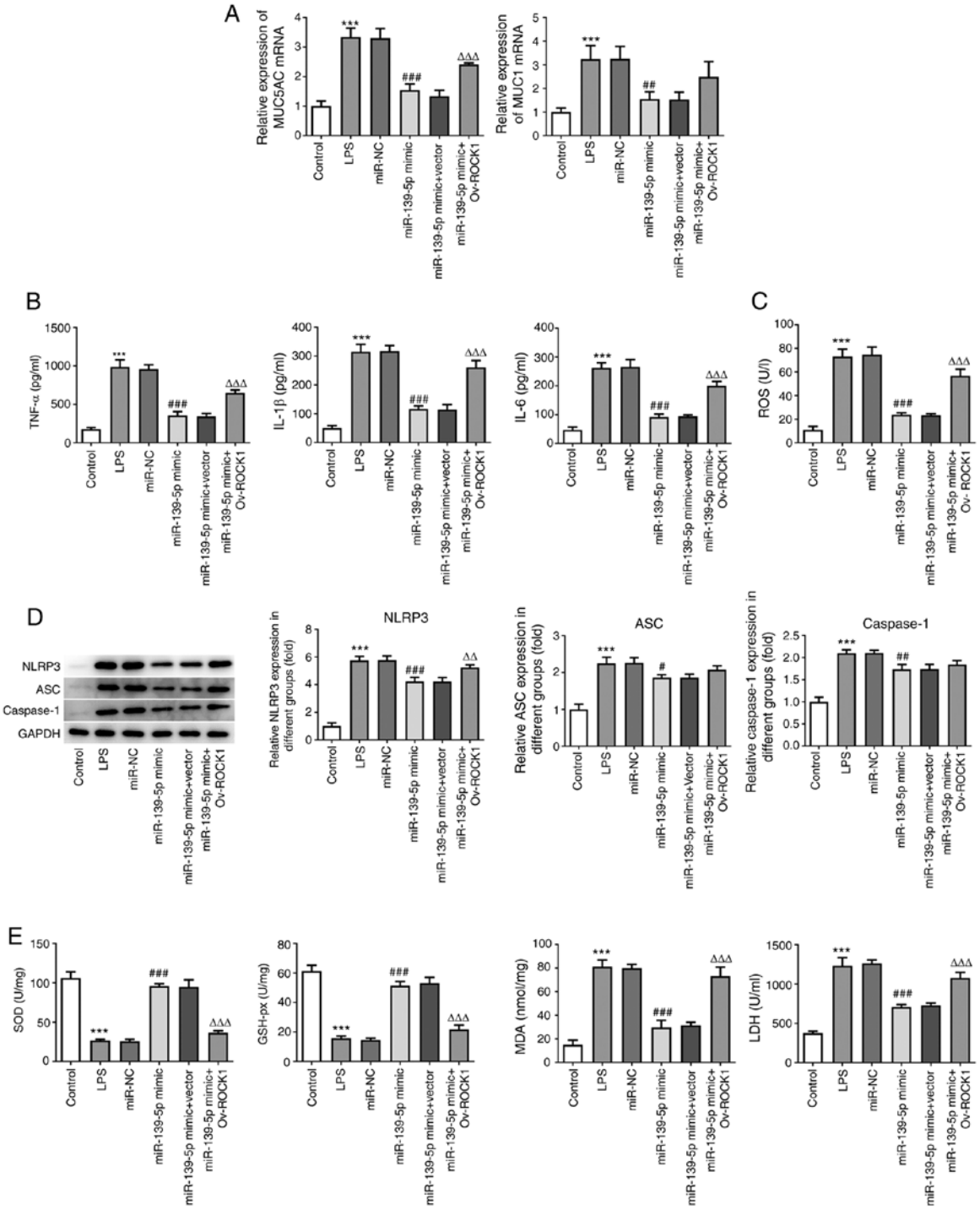

Figure 6. miR-139-5p overexpression inhibits LPS-induced inflammation and oxidative stress via targeting ROCK1 in NHBEs. NHBEs were divided into six groups: Control, LPS, LPS plus miR-NC mimics, LPS plus miR-139-5p mimics, LPS plus miR-139-5p mimics and empty vector, and LPS plus miR-139-5p mimics and Ov-ROCK1. (A) Relative mRNA expressions of MUC5AC and MUC1 were measured using RT-qPCR. (B) Proinflammatory cytokine levels in the treated NHBEs were examined using ELISA. (C) ROS levels in different groups. (D) Expression levels of NLRP3, ASC and caspase-1 in the treated NHBEs were examined using western blotting. (E) SOD, GSH-px and LDH activities and MDA levels were determined using commercial assay kits. Data are presented as the mean ± standard deviation. ***P<0.001 vs. control; $^{\#}$P<0.01, $^{\#\#}$P<0.005 and $^{\#\#\#}$P<0.001 vs. miR-NC; $^{\Delta\Delta}$P<0.005 and $^{\Delta\Delta\Delta}$P<0.001 vs. miR-139-5p mimics + Vector. ROCK1, Rho-associated kinase 1; miR, microRNA; RT-qPCR, reverse transcription-quantitative PCR; NHBEs, normal human bronchial epithelial cells; Ov, overexpression; SOD, superoxide dismutase; MDA, malondialdehyde; LDH, lactate dehydrogenase; GSH-px, glutathione peroxidase; LPS, lipopolysaccharide; NC, negative control; MUC, mucin; NLRP3, NLR family pyrin domain containing 3; ASC, apoptosis-associated speck-like protein containing a CARD.

miR-139-5p expression was significantly downregulated and positively correlated with ROCK1 expression during Ewing sarcoma progression (35). Moreover, the lncRNA X-inactive specific transcript was found to sponge miR-139-5p, thereby reducing the levels of ROCK1 (36). In the present study, miR-139-5p expression was reduced in the mice with sepsis-induced lung injury, whereas ROCK1 expression was significantly increased.

Further investigations on the role of miR-139-5p and targeting of ROCK1 in sepsis-induced lung injury were

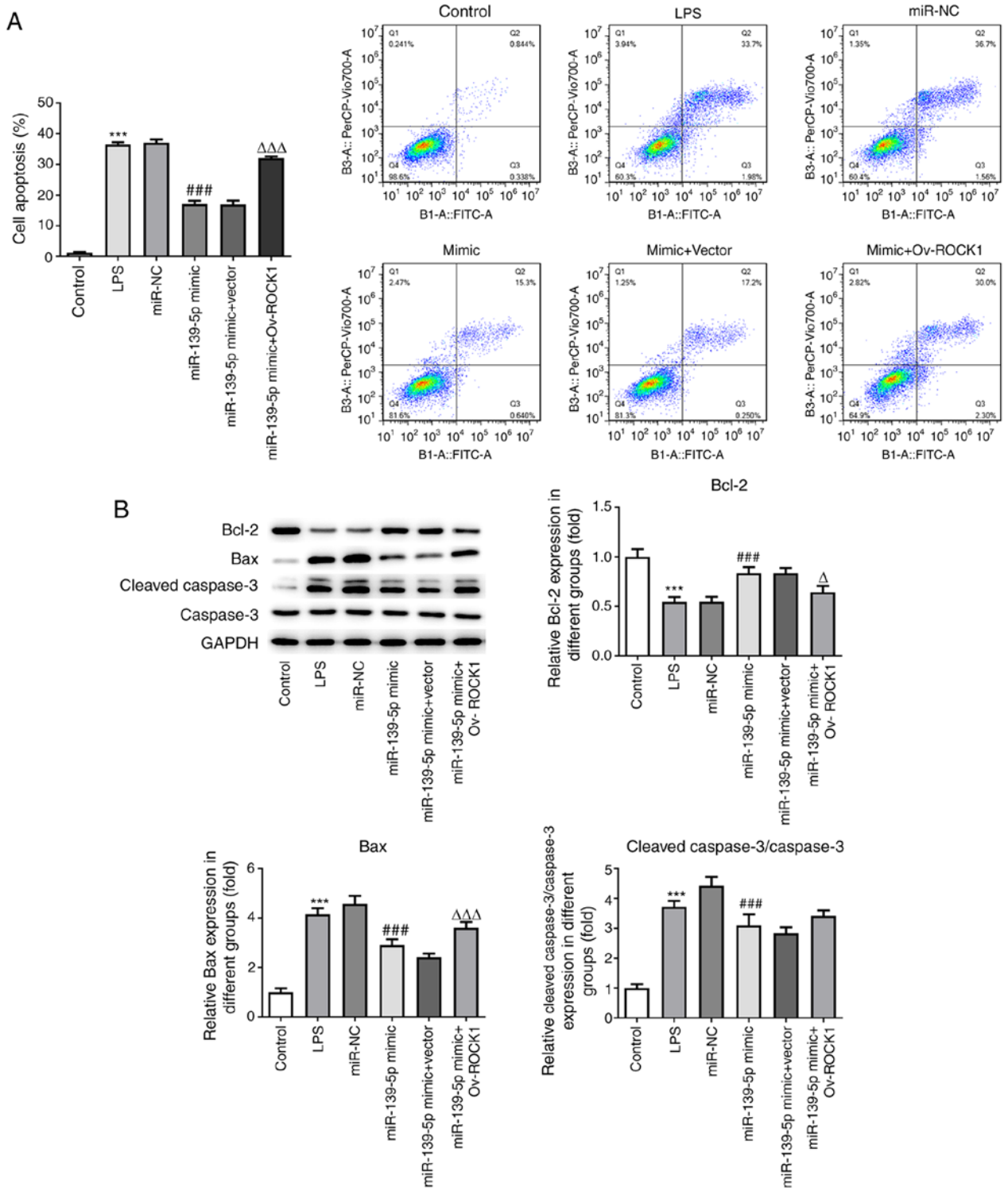

Figure 7. miR-139-5p overexpression reduces LPS-induced apoptosis by targeting ROCK1 in NHBEs. (A) Proportion of apoptotic cells among transfected NHBEs was determined using flow cytometry. (B) Expression levels of Bax, Bcl-2, cleaved caspase-3 and caspase-3 in the treated NHBEs were determined using western blotting (left, representative blots; right, densitometry analysis). Data are presented as the mean ± standard deviation. ***P<0.001 vs. control; $^{###}$P<0.001 vs. miR-NC; $^{\Delta}$P<0.01 and $^{\Delta\Delta\Delta}$P<0.001 vs. miR-139-5p mimics + Vector. NHBEs, normal human bronchial epithelial cells; ROCK1, Rho-associated kinase 1; miR, microRNA; LPS, lipopolysaccharide; NC, negative control; Ov, overexpression.

performed using LPS-treated NHBEs *in vitro*. Treatment with LPS resulted in a significant increase in the levels of inflammatory cytokines, oxidative stress and apoptosis in NHBEs compared with the untreated cells. Overexpression of miR-139-5p reversed these trends by decreasing the expression of ROCK1 in NHBEs.

In conclusion, miR-139-5p alleviated sepsis-induced proinflammatory cytokine production, oxidative stress and apoptosis induced by ALI via downregulation of ROCK1 expression levels. Therefore, the findings of the present study highlight miR-139-5p as a potential therapeutic target for the management of sepsis-induced ALI.

Acknowledgements

Not applicable.

Funding

The present study was supported by the Social Development Projects of Jiangsu Province (grant no. BE2017720).

Availability of data and materials

The datasets used and/or analyzed during the current study are available from the corresponding author on reasonable request.

Authors' contributions

SN primarily designed the protocol; XZ wrote the manuscript for this study and analyzed the data; MW and ZS performed the animal experiments; SZ, WZ and ZY performed the *in vitro* experiments; ZY and XH were involved in the coordination of experiments and data analysis. All authors read and approved the final manuscript. SN and XZ confirm the authenticity of all the raw data.

Ethics approval and consent to participate

All animals were handled in accordance with guidelines approved by the Experimentation Ethics Review Committee of Nanjing University (approval no. L2019320).

Patient consent for publication

Not applicable.

Competing interests

The authors declare that they have no competing interests.

References

1. Cecconi M, Evans L, Levy M and Rhodes A: Sepsis and septic shock. Lancet 392: 75-87, 2018.
2. Vincent JL, Marshall JC, Namendys-Silva SA, François B, Martin-Loeches I, Lipman J, Reinhart K, Antonelli M, Pickkers P, Njimi H, *et al*: Assessment of the worldwide burden of critical illness: The intensive care over nations (ICON) audit. Lancet Respir Med 2: 380-386, 2014.
3. Singer BH, Dickson RP, Denstaedt SJ, Newstead MW, Kim K, Falkowski NR, Erb-Downward JR, Schmidt TM, Huffnagle GB and Standiford TJ: Bacterial dissemination to the brain in Sepsis. Am J Respir Crit Care Med 197: 747-756, 2018.
4. Merx MW and Weber C: Sepsis and the heart. Circulation 116: 793-802, 2007.
5. Meneses G, Cardenas G, Espinosa A, Rassy D, Pérez-Osorio IN, Bárcena B, Fleury A, Besedovsky H, Fragoso G and Sciutto E: Sepsis: Developing new alternatives to reduce neuroinflammation and attenuate brain injury. Ann N Y Acad Sci 1437: 43-56, 2019.
6. Hato T, Maier B, Syed F, Myslinski J, Zollman A, Plotkin Z, Eadon MT and Dagher PC: Bacterial sepsis triggers an antiviral response that causes translation shutdown. J Clin Invest 129: 296-309, 2019.
7. Fowler AA III, Truwit JD, Hite RD, Morris PE, DeWilde C, Priday A, Fisher B, Thacker LR II, Natarajan R, Brophy DF, *et al*: Effect of vitamin C infusion on organ failure and biomarkers of inflammation and vascular injury in patients with sepsis and severe acute respiratory failure: The CITRIS-ALI randomized clinical trial. JAMA 322: 1261-1270, 2019.
8. Fernandez FG, Kosinski AS, Furnary AP, Onaitis M, Kim S, Habib RH, Tong BC, Cowper P, Boffa D, Jacobs JP, *et al*: Differential effects of operative complications on survival after surgery for primary lung cancer. J Thorac Cardiovasc Surg 155: 1254-1264.e1, 2018.
9. Vazquez-Medina JP, Tao JQ, Patel P, Bannitz-Fernandes R, Dodia C, Sorokina EM, Feinstein SI, Chatterjee S and Fisher AB: Genetic inactivation of the phospholipase A2 activity of peroxiredoxin 6 in mice protects against LPS-induced acute lung injury. Am J Physiol Lung Cell Mol Physiol 316: L656-L668, 2019.
10. Guo RF and Ward PA: Role of oxidants in lung injury during sepsis. Antioxid Redox Signal 9: 1991-2002, 2007.
11. Yi L, Chang M, Zhao Q, Zhou Z, Huang X, Guo F and Huan J: Genistein-3'-sodium sulphonate protects against lipopolysaccharide-induced lung vascular endothelial cell apoptosis and acute lung injury via BCL-2 signalling. J Cell Mol Med 24: 1022-1035, 2020.
12. Swisher EM, Lin KK, Oza AM, Scott CL, Giordano H, Sun J, Konecny GE, Coleman RL, Tinker AV, O'Malley DM, *et al*: Rucaparib in relapsed, platinum-sensitive high-grade ovarian carcinoma (ARIEL2 Part 1): An international, multicentre, open-label, phase 2 trial. Lancet Oncol 18: 75-87, 2017.
13. Hennessy EJ, Parker AE and O'Neill LA: Targeting Toll-like receptors: Emerging therapeutics? Nat Rev Drug Discov 9: 293-307, 2010.
14. Seeley JJ, Baker RG, Mohamed G, Bruns T, Hayden MS, Deshmukh SD, Freedberg DE and Ghosh S: Induction of innate immune memory via microRNA targeting of chromatin remodelling factors. Nature 559: 114-119, 2018.
15. Gotts JE and Matthay MA: Sepsis: Pathophysiology and clinical management. BMJ 353: i1585, 2016.
16. Zhu M, Zhang W, Ma J, Dai Y, Zhang Q, Liu Q, Yang B and Li G: MicroRNA-139-5p regulates chronic inflammation by suppressing nuclear factor-κB activity to inhibit cell proliferation and invasion in colorectal cancer. Exp Ther Med 18: 4049-4057, 2019.
17. Qu Y, Wu J, Chen D, Zhao F, Liu J, Yang C, Wei D, Ferriero DM and Mu D: MiR-139-5p inhibits HGTD-P and regulates neuronal apoptosis induced by hypoxia-ischemia in neonatal rats. Neurobiol Dis 63: 184-193, 2014.
18. Huang N, Guo W, Ren K, Li W, Jiang Y, Sun J, Dai W and Zhao W: LncRNA AFAP1-AS1 Supresses miR-139-5p and promotes cell proliferation and chemotherapy resistance of non-small cell lung cancer by competitively upregulating RRM2. Front Oncol 9: 1103, 2019.
19. Wang Y, Wang X, Liu W and Zhang L: Role of the Rho/ROCK signaling pathway in the protective effects of fasudil against acute lung injury in septic rats. Mol Med Rep 18: 4486-4498, 2018.
20. Ruiz S, Vardon-Bounes F, Merlet-Dupuy V, Conil JM, Buléon M, Fourcade O, Tack I and Minville V: Sepsis modeling in mice: Ligation length is a major severity factor in cecal ligation and puncture. Intensive Care Med Exp 4: 22, 2016.
21. Zhuo Y, Li D, Cui L, Li C, Zhang S, Zhang Q, Zhang L, Wang X and Yang L: Treatment with 3,4-dihydroxyphenylethyl alcohol glycoside ameliorates sepsis-induced ALI in mice by reducing inflammation and regulating M1 polarization. Biomed Pharmacother 116: 109012, 2019.
22. Matute-Bello G, Downey G, Moore BB, Groshong SD, Matthay MA, Slutsky AS and Kuebler WM: An official American Thoracic Society workshop report: Features and measurements of experimental acute lung injury in animals. Am J Respir Cell Mol Biol 44: 725-738, 2011.
23. Livak KJ and Schmittgen TD: Analysis of relative gene expression data using real-time quantitative PCR and the 2(-Delta Delta C(T)) Method. Methods 25: 402-408, 2001.
24. Shang G, Jin Y, Zheng Q, Shen X, Yang M, Li Y and Zhang L: Histology and oncogenic driver alterations of lung adenocarcinoma in Chinese. Am J Cancer Res 9: 1212-1223, 2019.
25. Englert JA, Bobba C and Baron RM: Integrating molecular pathogenesis and clinical translation in sepsis-induced acute respiratory distress syndrome. JCI Insight 4: e124061, 2019.
26. Konduri K, Gallant JN, Chae YK, Giles FJ, Gitlitz BJ, Gowen K, Ichihara E, Owonikoko TK, Peddareddigari V, Ramalingam SS, *et al*: EGFR fusions as novel therapeutic targets in lung cancer. Cancer Discov 6: 601-611, 2016.
27. Dejager L, Pinheiro I, Dejonckheere E and Libert C: Cecal ligation and puncture: The gold standard model for polymicrobial sepsis? Trends Microbiol 19: 198-208, 2011.
28. Hong HC, Chuang CH, Huang WC, Weng SL, Chen CH, Chang KH, Liao KW and Huang HD: A panel of eight microRNAs is a good predictive parameter for triple-negative breast cancer relapse. Theranostics 10: 8771-8789, 2020.

29. Du F, Cao T, Xie H, Li T, Sun L, Liu H, Guo H, Wang X, Liu Q, Kim T, *et al*: KRAS Mutation-Responsive miR-139-5p inhibits colorectal cancer progression and is repressed by Wnt Signaling. Theranostics 10: 7335-7350, 2020.
30. Xiu D, Liu L, Cheng M, Sun X and Ma X: Knockdown of lncRNA TUG1 enhances radiosensitivity of prostate cancer via the TUG1/miR-139-5p/SMC1A Axis. Onco Targets Ther 13: 2319-2331, 2020.
31. Wen J, Wang G, Xie X, Lin G, Yang H, Luo K, Liu Q, Ling Y, Xie X, Lin P, *et al*: Prognostic value of a Four-miRNA signature in patients with lymph node positive locoregional esophageal squamous cell carcinoma undergoing complete surgical resection. Ann Surg 273: 523-531, 2021.
32. Pajic M, Froio D, Daly S, Doculara L, Millar E, Graham PH, Drury A, Steinmann A, de Bock CE, Boulghourjian A, *et al*: MiR-139-5p modulates radiotherapy resistance in breast cancer by repressing multiple gene networks of DNA repair and ROS defense. Cancer Res 78: 501-515, 2018.
33. Zou F, Mao R, Yang L, Lin S, Lei K, Zheng Y, Ding Y, Zhang P, Cai G, Liang X and Liu J: Targeted deletion of miR-139-5p activates MAPK, NF-κB and STAT3 signaling and promotes intestinal inflammation and colorectal cancer. FEBS J 283: 1438-1452, 2016.
34. Li C, Ma D, Yang J, Lin X and Chen B: MiR-202-5p inhibits the migration and invasion of osteosarcoma cells by targeting ROCK1. Oncol Lett 16: 829-834, 2018.
35. Roberto GM, Delsin LEA, Vieira GM, Silva MO, Hakime RG, Gava NF, Engel EE, Scrideli CA, Tone LG and Brassesco MS: ROCK1-PredictedmicroRNAs dysregulation contributes to tumor progression in ewing sarcoma. Pathol Oncol Res 26: 133-139, 2020.
36. Tian K, Sun D, Chen M, Yang Y, Wang F, Guo T and Shi Z: Long Noncoding RNA X-Inactive specific transcript facilitates cellular functions in melanoma via miR-139-5p/ROCK1 Pathway. Onco Targets Ther 13: 1277-1287, 2020.